EUROPEAN ORGANIZATION FOR NUCLEAR RESEARCH

CERN – PS DIVISION

CERN/PS 2002-075 (PP)

EFFECTS OF THERMAL SHOCKS ON THE RELEASE OF RADIOISOTOPES AND ON MOLTEN METAL TARGET VESSELS *

G. Arnau, M. Benedikt, R. Catherall, G. Cyvogt, A. Fabich, U. Georg, S. Gilardoni, O. Jonsson, J. Lettry†, H. Ravn, S. Sgobba, and the ISOLDE collaboration
CERN, Geneva, Switzerland.
G. Bauer, H. Brucherstseifer, T. Graber, C. Güdermann, L. Ni, R. Rastani
PSI Würenlingen, Switzerland.

Abstract

The ISOLDE pulsed proton beam peak power amounts to 500 MW during the 2.4 μs proton pulse. The fraction of the proton pulse energy deposited in the target material is at the origin of severe thermal shocks. Quantitative measurement of their effect on the release of radioelements from ISOLDE targets was obtained by comparison of release profiles measured under different proton beam settings.
The thermal shock induced in liquids (Pb, Sn, La) lead to mechanical failure of ISOLDE molten metal target vessels. Failure analysis is presented and discussed in the light of the response of mercury samples submitted to the ISOLDE beam and monitored by high-speed optical systems.

Paper presented at the 14th International Conference on Electromagnetic Isotope Separators and Techniques Related to their Application, 6-10 May, 2002, Victoria, B.C., Canada

Geneva, Switzerland
26 September 2002

† e-mail: Jacques.lettry@cern.ch
* Supported by the EU RTD projects EURISOL (HPRI-CT-1999-50001) and TARGISOL (HPRI-CT-2001-50033).

EFFECTS OF THERMAL SHOCKS ON THE RELEASE OF RADIOISOTOPES AND ON MOLTEN METAL TARGET VESSELS *

J. Lettry†, G. Arnau, M. Benedikt, S. Gilardoni, R. Catherall, U. Georg, G. Cyvogt, A. Fabich, O. Jonsson, H. Ravn, S. Sgobba, and the ISOLDE collaboration
CERN, Geneva, Switzerland.
G. Bauer, H. Brucherstseifer, T. Graber, C. Güdermann, L. Ni, R. Rastani
PSI Würenlingen, Switzerland.

The ISOLDE pulsed proton beam peak power amounts to 500 MW during the 2.4 μs proton pulse. The fraction of the proton pulse energy deposited in the target material is at the origin of severe thermal shocks. Quantitative measurement of their effect on the release of radioelements from ISOLDE targets was obtained by comparison of release profiles measured under different proton beam settings.

The thermal shock induced in liquids (Pb, Sn, La) lead to mechanical failure of ISOLDE molten metal target vessels. Failure analysis is presented and discussed in the light of the response of mercury samples submitted to the ISOLDE beam and monitored by high-speed optical systems.

Release of radioisotopes under pulsed proton beam conditions

The pulsed proton beam of the ISOLDE facility [1] offers a unique opportunity to study the release of the produced radioisotopes by monitoring their time structure. As an immediate result, the decay losses in the target is extracted from these data and, together with the ion-source efficiency and geometrical factors accounting for the matching of the target geometry to the proton beam size, is used to objectively compare production yields and cross sections [2,3]. These measurements build a basis for theoretical diffusion and effusion studies on existing target and ion-source systems [4-7]. Therefore, it opens the way towards the optimization of the target materials and overall geometry that are required for the efficient production of short-lived isotopes and for the design of high power targets. However, the transient temperature rise during proton impact, the cyclic irradiation conditions (typical periodicity of 14.4s, adjustable between 7.2 s and 5×14.4 s) and the presence of radioisotopes produced by decay of precursors after proton impact heavily add complexity to the models. The aim of this section is to discuss the measurement of effects related to thermal shocks induced by the proton pulse.

The measurement of the release of ^{139}Cs and ^{224}Fr from a uranium carbide target equipped with a Nb surface ion-source are presented in Figure 1 for proton beam intensities of 3×10^{12} and 3×10^{13} protons per pulse (ppp). The point-to-point ratios of each measurement are presented in Figure 2. Linear normalization by the proton pulse intensity and for the increasing proton beam size with intensity was applied. As expected, the release obtained with high intensity proton pulses is faster shortly after beam impact. For francium and cesium, the ratio of release profiles measured with nominal and one tenth of nominal proton pulse intensity fit an exponential with a time constant of 0.4 s that is interpreted as the evolution of the temperature transient. These elements were chosen specifically with a release time of the

† e-mail: Jacques.lettry@cern.ch
* Supported by the EU RTD projects EURISOL (HPRI-CT-1999-50001) and TARGISOL (HPRI-CT-2001-50033).

order of the proton pulse repetition rate (14.4 s). The fraction still within the target at the next proton impact will therefore also be heated by the following pulse and contributes to the observed difference.

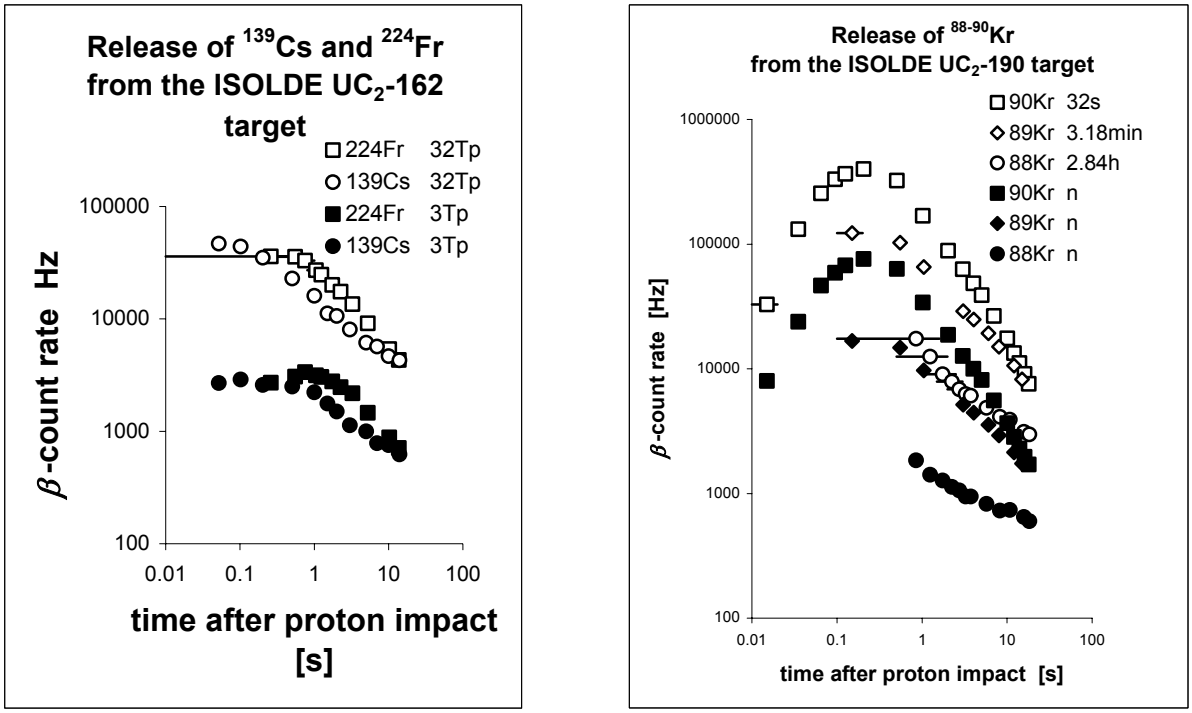

Figure 1. Release data of ^{139}Cs, ^{224}Fr and $^{88\text{-}90}$Kr from ISOLDE Uranium carbide targets measured via 4 ms (Cs), 500 ms (Fr) and 4 to 1500 ms (Kr) collections followed by β-counting during 1 s. For ^{139}Cs and ^{224}Fr, the intensities of the 1GeV-proton pulse were 3 and 32 Tp (1Tp=10^{12} protons). For the krypton isotopes, the fission of ^{238}U was induced by 1.4 GeV protons (20 Tp) or via the neutrons (n) generated in a nearby placed W-rod irradiated by 1.4 GeV protons (20 Tp).

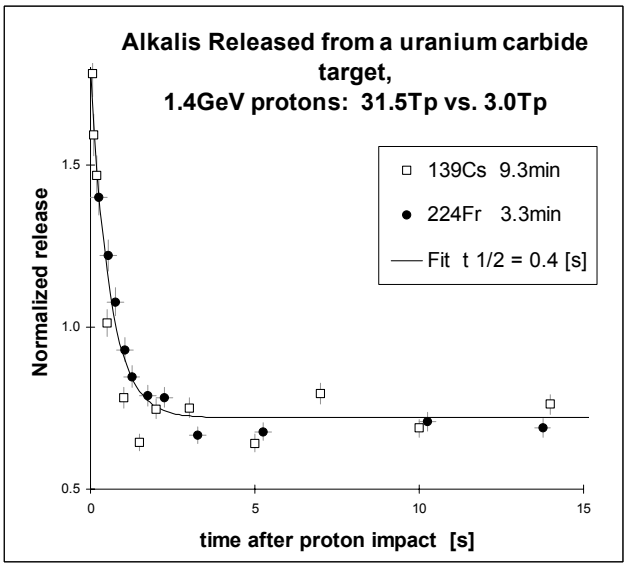

Figure 2. Effect of the proton pulse intensity on the release of ^{139}Cs and ^{224}Fr from a uranium carbide target. For each isotope, the release was measured with proton pulse intensities of 3.2×10^{13}ppp and 3×10^{12}ppp. The point-to-point ratio of the samples activities are normalized to their respective proton pulse intensities corrected with a geometrical factor accounting for the increase of the proton beam size with pulse intensity. The error bars are statistical only and the horizontal line extends over the radioisotope collection time.

Krypton release data are presented in Figure 1 for a uranium carbide target equipped with a cold transfer line, a plasma ion-source and a neutron converter [8,9]. All measurements were recorded with 2×10^{13} ppp and the thermal shock was reduced by inducing fission via neutrons instead of high-energy protons. The neutrons were generated by 1.4 GeV protons impacting on a 150 mm long 12.5 mm diameter W-rod placed close to the target. The ratios presented in Figure 3 ($^{88\text{-}90}$Kr) are normalized to the average of the data recorded later than 10 s after beam impact to account for the difference in production cross section.

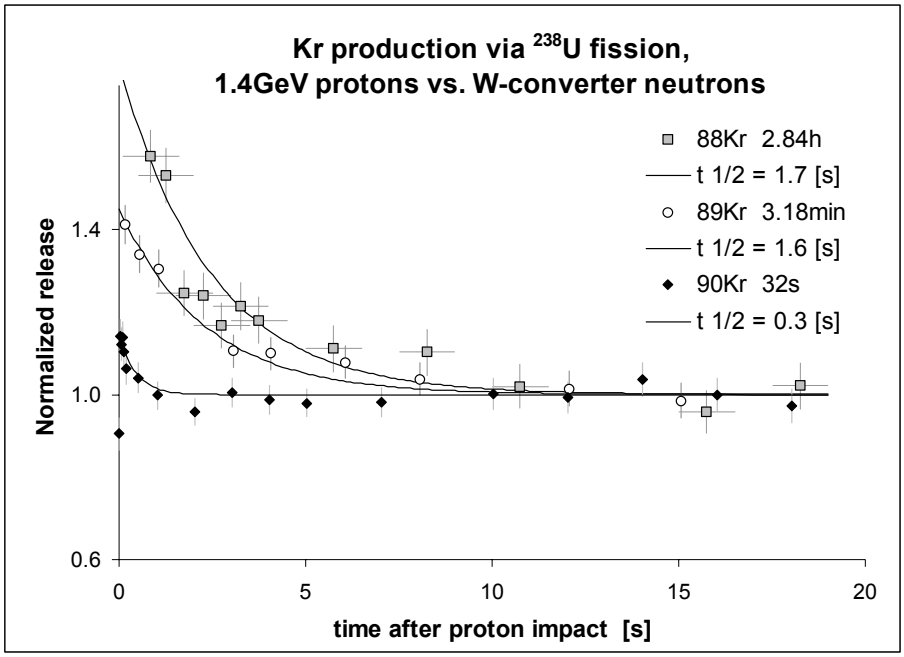

Figure 3. Comparison of the time structure of the release of the $^{88\text{-}90}$Kr. The fission products were generated by high-energy proton interactions or by neutron induced fission of ^{238}U in the same ISOLDE uranium carbide target. The measurements are normalized to account for different cross sections for each isotope, the average of the point-to-point ratios is normalized to 1 for all measurements collected later than 10 s after proton impact where thermal equilibrium is likely to be reached. The error bars are statistical only and the horizontal line extends over the radioisotope collection time.

The energy depositions in the target and in the converter were simulated using MARS [10-13] interfaced with MCNP4C [14,15]. The maximum energy density of the hadronic cascade induced by a 30 Tp (1 Tp = 10^{12} protons) 1 GeV proton pulse is 29.6 J/g for direct irradiation and 0.1 J/g while protons are impacting on the neutron converter.

The three Kr isotopes show the exponential behavior mentioned for Cs and Fr but quite different time constants and amplitudes. It is a known effect of cold transfer lines that precursor isotopes ($^{88\text{-}90}$Br) frozen in the cold transfer line do contribute to the production of the noble gas. However, the direct relation to this observation and its analysis requires a precise knowledge of the cross sections.

In ISOLDE uranium carbide targets, the intensity of the released isotopes increases up to a factor of 1.8 during the temperature transient immediately after beam impact. Thus, effusion studies based on such release data should account for the effect of temperature transients. This "acceleration" of the release is fortunately concomitant to the maximum of the release of short-lived alkalis and noble gases. However, the geometrical factor (84% of the protons hitting the target) for high intensity proton pulses does not reproduce the observed yield ratios of 0.63 (Fr) and 0.65(Cs). The effect is more pronounced for the longer-lived elements of an isotopic chain both in amplitude and duration, thus showing that a non-negligible fraction of the effect is due to the presence of atoms remaining from previous pulses.

Thermal shocks in ISOLDE molten metal targets

The consequences of thermal shocks induced by a pulsed proton beam [16,17] on ISOLDE molten metal targets were addressed as follows [18]. The baffles installed in the transfer line prevent liquid metal splashes to reach the ion-source, while a temperature controlled condensation helix prevent vapor bursts. The reinforcement of the target containers successfully increased their lifetime, and the lengthening of the proton pulse from 2.4 μs to ~20 μs coupled to a doubling of the beam size [19-21] raised the proton intensity threshold of the splashes.

While the molten metal targets are in reliable operational condition, the proton beam interaction still generates splashes within them. The effect of the change of the accelerator harmonic number (from 5 to 1) and of the newly available 1.4 GeV proton beam energy should be addressed. This section describes the fatigue and corrosion observed on the proton beam window of a lead target, and the measurements of molten metal splash velocities.

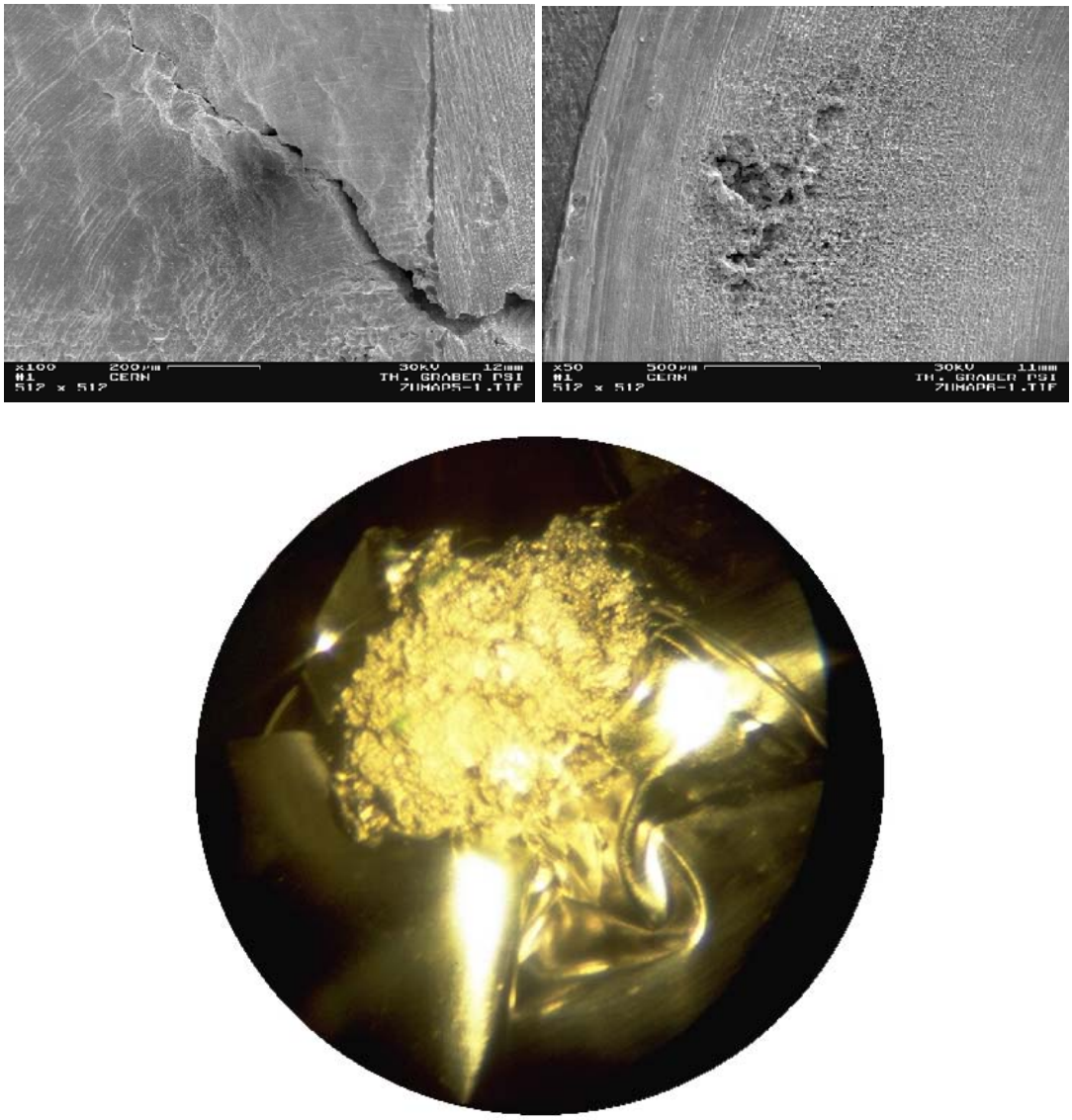

Figure 4. a) Inner side of the Ta-window of the Pb-043 ISOLDE molten lead target after etching of the remaining lead. The thermal stress induced crack following the grain boundaries is clearly visible. b) The regular machining tracks are visible around the typical corrosion pattern of cavitation found on a 0.5 by 1 mm spot. c) deformation of the proton beam entrance window of a tantalum target container. The cauliflower build up is a result of 1 Mcycles focused proton beam (5×7mm FWHM) on a 2100° Ta-foil target.

The inner side of the Ta-window of the ISOLDE molten lead target Pb-043 is presented in Figure 4. After etching of the remaining lead with 100 ml 1:3 nitric acid + 1 g tartaric acid, a thermal stress induced crack was visible (0.05 mm by 1 mm). The crack follows the Ta grain boundaries and thus shows the characteristic shape of its thermo mechanic cycling origin. The regular machining tracks are clearly visible around a 0.5 by 1 mm spot marked by the typical corrosion pattern of cavitation. The e-beam welded tantalum container of Pb-043 was operated at 720°. The proton beam size was 7×11 mm FWHM and its intensity was 6.5×10^{12} ppp. Migration of Fe impurities was observed at the Ta grain boundaries and 5 μm cracks were scattered in the bulk material.

As liquid metals may be quite difficult to investigate, the non-wetting and room temperature liquid, mercury, was chosen to measure splash velocities, thus using it as a "generic" molten metal test case. The mercury was filled into a thimble (12 mm diameter 12 mm height) or a trough (12×12×60mm) machined within a 316LN stainless steel frame mounted between two quartz windows. This assembly was supported (within tight confinement) by a standard ISOLDE target base and placed on the ISOLDE GPS front-end. The shadow of the splashing mercury was monitored with a high-speed camera (8000 frames/s, 25 μs shutter), followed by image processing. The output of a typical mercury trough measurement is presented in Figure 5, (ISOLDE proton pulse of 2×10^{13} ppp within 2.4 μs). The mercury velocity reaches above 30 m/s in a region between 0 and 20 mm behind the beam entrance window and 15 m/s at the end of the 60 mm long thimble. To mention an order of magnitude, this corresponds to a 108 km/h jet that would reach 45 m heights under vacuum.

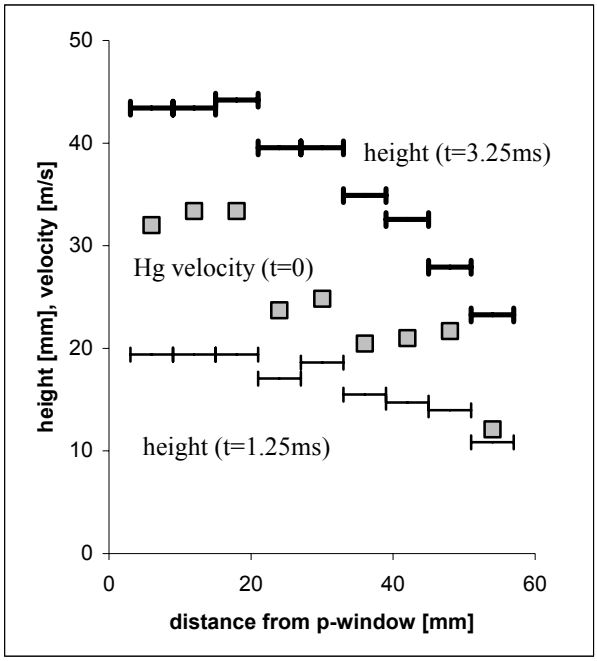

Figure 5. Hg splashing out of the 12×12×60 mm trough. The lines indicate the height of the mercury 1.25 and 3.25 ms after the impact of a pulse of 2×10^{13} protons. The initial velocities (t=0) presented result from the average movement recorded in a 6 mm band perpendicular to the trough surface.

The scaling laws with various proton beam parameters (intensity, beam size, time structure of the proton beam) were measured [22,23] and are the subject of a separate publication. The extrapolation of these measurements to other liquid metals can be estimated via the material constants and hadronic cascade energy deposition profiles. For fixed proton beam conditions, the splash velocities only depend on the proton beam induced thermal stress and on the density proportional inertia.

The thermal stress resulting from a sudden energy deposition in a liquid metal is described by: $s = \Delta T \cdot \alpha / \kappa$, where $\Delta T = dE/c_p$ is the temperature elevation, dE the energy deposited by the proton beam, c_p the heat capacity of the liquid metal, α its dilatation coefficient and k_s its compressibility (more specifically the isentropic compressibility extracted from the relation $k_s = 1/\rho u^2$, where ρ is the density and u the speed of sound in the molten metal). These parameters [24,25] are summarized in Table 1.

Table 1. Comparison of the material properties involved in the computation of the proton induced thermal stress in molten metals and their containment or converter material (tantalum). The value of dE is the maximum energy density of the hadronic cascade induced by a 3×10^{13} ppp proton pulse (1 GeV protons, $\sigma_x=\sigma_y=2.2$ mm, simulated using MARS [10-13] interfaced with MCNP4C [14,15]).
For solid Ta (*), the stress is given by $s = \Delta T \cdot \alpha \cdot E_Y/(1-(n-1)\nu)$, where, n stands for the number of dimension (n = 3 for the Ta-converter), E_Y is Young's Modulus (280×10^9 N/m^2), and ν the Poisson ratio (0.34). The values quoted are the one of annealed tantalum at room temperature.

	ρ	α	c_p	dE	dT	k_s	s
	g/cm^3		J/g/K	J/g	K	m^2/N	MPa
Hg	13.3	1.83×10^{-4} $_{vol}$	0.139	26.4	190	2.63×10^{-11}	1300
Pb	10.7	1.23×10^{-4} $_{vol}$	0.145	26.5	185	2.83×10^{-11}	795
Sn	7.0	0.88×10^{-4} $_{vol}$	0.250	28.8	115	2.34×10^{-11}	430
La	6.0	3.98×10^{-4} $_{vol}$	0.058	27.9	485	3.36×10^{-11}	5700
Ta	16.6	0.065×10^{-4} $_{lin}$	0.14	32.4	231		* 860

Neglecting fluid dynamics issues and the potential influence of the molten metal container (2-10 mm stainless steel for Hg and 0.5 to 4 mm tantalum for ISOLDE targets), we define s/ρ as a figure of merit to compare proton generated splashes in different liquid metals. This indicates that lead and tin should show effects comparable to the one of mercury while lanthanum should react much more according to its larger dilatation coefficient and lower heat capacity. It is no surprise that a baffle system is mandatory in ISOLDE molten metal targets. The stress induced in the tantalum proton beam window is sufficient to generate the fatigue effects observed in the lead target containers. Further more, this is the origin of the destruction of high temperature tantalum containers (operated with focused proton beam of 5×7 mm FWHM and above 2100°) presented in figure 4 and of the deformation the neutron converters presented in [9].

References

[1] ISOLDE PS Booster Facility at CERN: Experiments with slow radioactive beams, Nucl. Phys. News, Vol 3, No 2, 1993.

[2] J. Lettry, R. Catherall, P. Drumm, P. Van Duppen, A. Evensen, G. Focker, A. Jokinen, O. Jonsson, E. Kugler, H. Ravn and the ISOLDE collaboration.
Nucl. Instrum. and Meth. **B** 126 (1997) 130-134.

[3] J. Lettry, R. Catherall, G. Cycoct, P. Drumm, A. Evensen, M. Lindroos, O.C. Jonsson, E. Kugler, J. Obert, J.C. Puteaux, J. Sauvage, K. Schindl, H. Ravn, E.Wildner and the ISOLDE Collaboration, Nuclear instruments and Methods in Physics Research **B** 126 (1997) 170.

[4] R. Bennett, Nuclear instruments and Methods in Physics Research **B** 126 (1997) 146.

[4] C. J. Densham, C. Thwaites, R. Bennett, Nuclear instruments and Methods in Physics Research **B** 126 (1997) 155.

[5] P. Drumm, J. Bennett, C. Densham, W. Evans, M. Holding, G. Murdoch, R. Catherall, A. Evensen, O. Jonsson, E. Kugler, J. Lettry, H. Ravn, O. Tengblad, P. Van Dippen, J.

Kay, D. Warner, M. Harder, C. Thwaites, J. Honsi, R. Page, J. Billowes, S. Freeman, I. Grant, S. Schwebel, G. Smith, C. Bishop, P. Walker and the ISOLDE collaboration. EMIS-XIII, Nucl. Instrum. and Meth. **B** 126 (1997) 121-124.
[6] J. R. J. Bennett, Uffe Bergmann , P. V. Drumm; J. Lettry, T. Nilsson, R. Catherall, O. C. Jonsson, H. L. Ravn, H. Simon, and the ISOLDE Collaboration, Conference proceeding RNB5 2000 Divonne, submitted to Esevier
[7] J.R.J. Bennett, these proceedings.
[8] U. Bergmann, these proceedings.
[9] R. Catherall, these proceedings.
[10] N.V. Mokhov, "The Mars Code System User's Guide", Fermilab-FN-628 (1995).
[11] N.V. Mokhov, "MARS Code Developments, Benchmarking and Applications", Fermilab-Conf-00-066 (2000).
[12] N.V. Mokhov, S.I. Striganov, A. Van Ginneken, S.G. Mashnik, A.J. Sierk and J. Ranft "MARS Code Developments", Fermilab-Conf-98/379 (1998); LANL Report LA-UR-98-5716 (1998); nucl-th/9812038 v2 16 Dec 1998.
[13] O.E. Krivosheev and N.V. Mokhov, "A New MARS and its Applications", Fermilab-Conf-98/43 (1998).
[14] J.S. Hendrics, "MCNP4C" LANL Memo X-5; JSH-2000-3
[15] J.F. Briesmesteir, ed. "MCNP - A General Montecarlo N-Particle Transport Code, Version 4C", LA-13709-M
[16] K. Skala, G.S. Bauer, ICANS-XIII, International Conference on Advanced Neutron Sources, PSI proceedings 95-02, 1995, 559.
[17] Y. Takeda, ESS 95-31,1995.
[18] J. Lettry, R. Catherall, P. Drumm, A. Evensen, O.C. Jonsson, E. Kugler, J. Obert, J.C. Puteaux, J. 4Sauvage, M. Toulemonde and the ISOLDE Collaboration, ICANS-XIII, International Conference on Advanced Neutron Sources, PSI proceedings 95-02, 1995, 595.
[19] G. Cyvogt, M. Lindroos and K. Schindl, Test of new optics for the ISOLDE line 28-29 March 1996, CERN PS/OP Note 96-14.
[20] G. Cyvogt, M. Lindroos, K. Schindl and R. Steerenberg, 1996, Summary of tests for the ISOLDE HRS and GPS lines, CERN PS/OP Note 96-15.
[21] G. Cyvogt, M. Lindroos, K. Schindl and E. Wildner, Staggered extraction of the four BOOSTER rings for ISOLDE : Beam test results and future perspectives. CERN PS/OP/Note 95-58, 16/10/95
[22] A. Fabich, J. Lettry, conference proceedings, Nufact 01 Tsukuba, Japan (2001), to be published in NIM A.
[23] J. Lettry, A. Fabich, conference proceedings, Nufact 02 London, England (July 2002) to be published.
[24] Smithells Metals refernce book, Butterworth 1976.
[25] G. Arnau, CERN EST/SM, 343886 2002.